Solar radiation

The sun as a source of energy

The sun is the main source of energy for the climate system, exceeding the next importat source (geothermal energy) by 4 orders of magnitude!

Sources of energy for the climate systems

• solar radiation	$1.74 \cdot 10^{17}$ W
• geothermal energy	$3.2 \cdot 10^{13}$ W
• anthropogenic energy generation	$1.0 \cdot 10^{13}$ W
• infrared emission by the full moon	$5.0 \cdot 10^{12}$ W
• solar radiation reflected by the full moon	$2.0 \cdot 10^{12}$ W
• radiation by the stars	$8.0 \cdot 10^{8}$ W

The structure of the sun

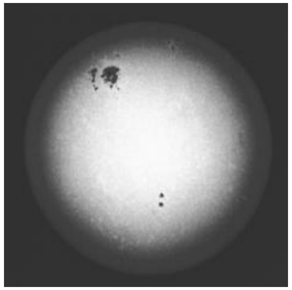

Photo by NASA

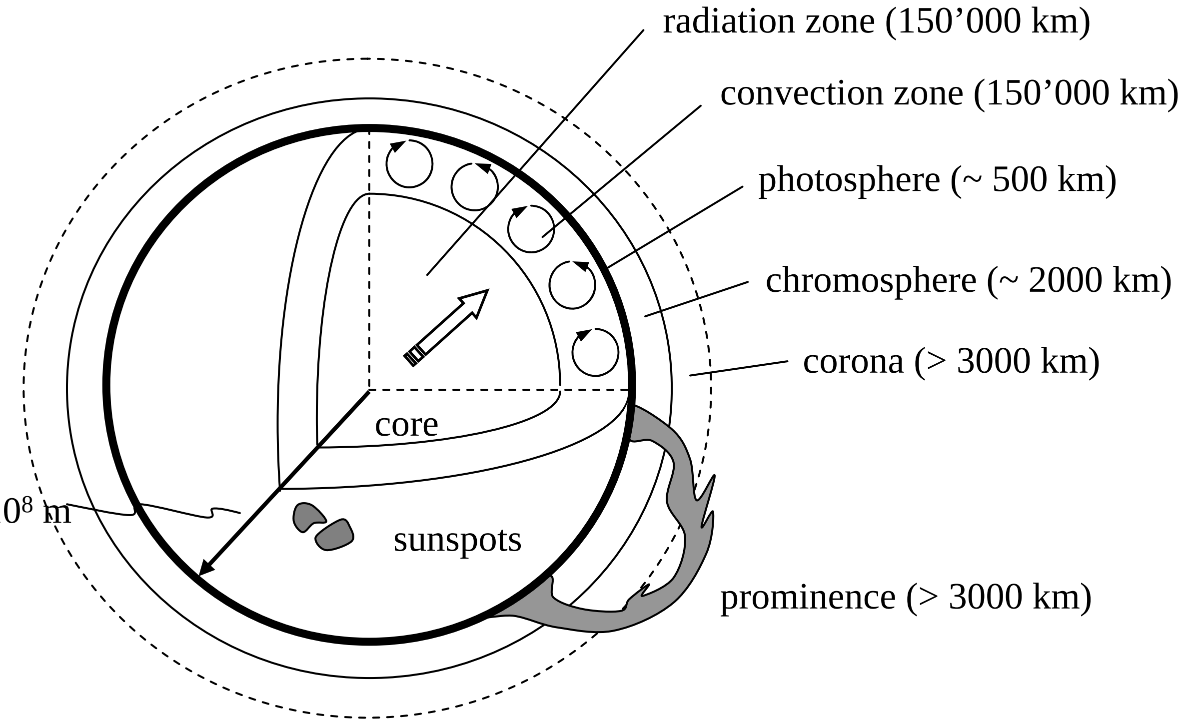

The visible region of the sun is called photosphere. Most of the radiation reaching the earth originates from this layer. Although the sun is a gaseous body, the photosphere is usually referred to as the surface of the sun. The temperature of this layer varies between 4000 and 8000 K. A temperature of 5800 K is required to explain the observed spectral distribution of the solar radiation (Planck curve).

The structure of the sun (2)

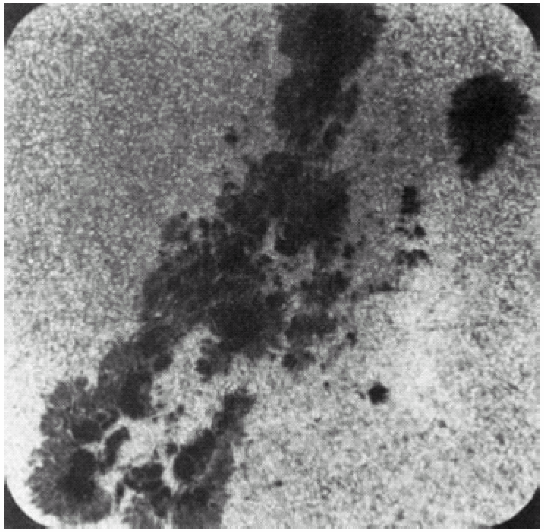

Fig. 2 A large sunspot group showing dark umbral and intermediate penumbral regions contrasted against the brighter surrounding photosphere. (Sacramento Peak Observatory, Association of Universities for Research in Astronomy, Inc.)

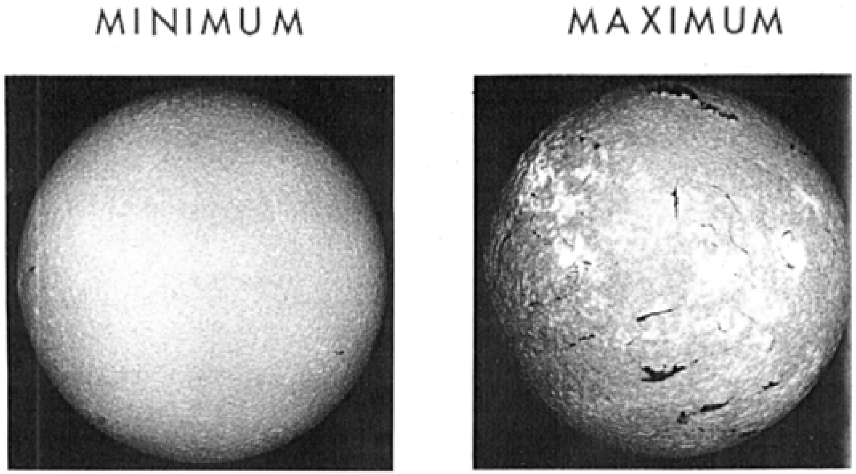

NATIONAL SOLAR OBSERVATORY / SACRAMENTO PEAK, N.M.

Spectrum of the solar radiation

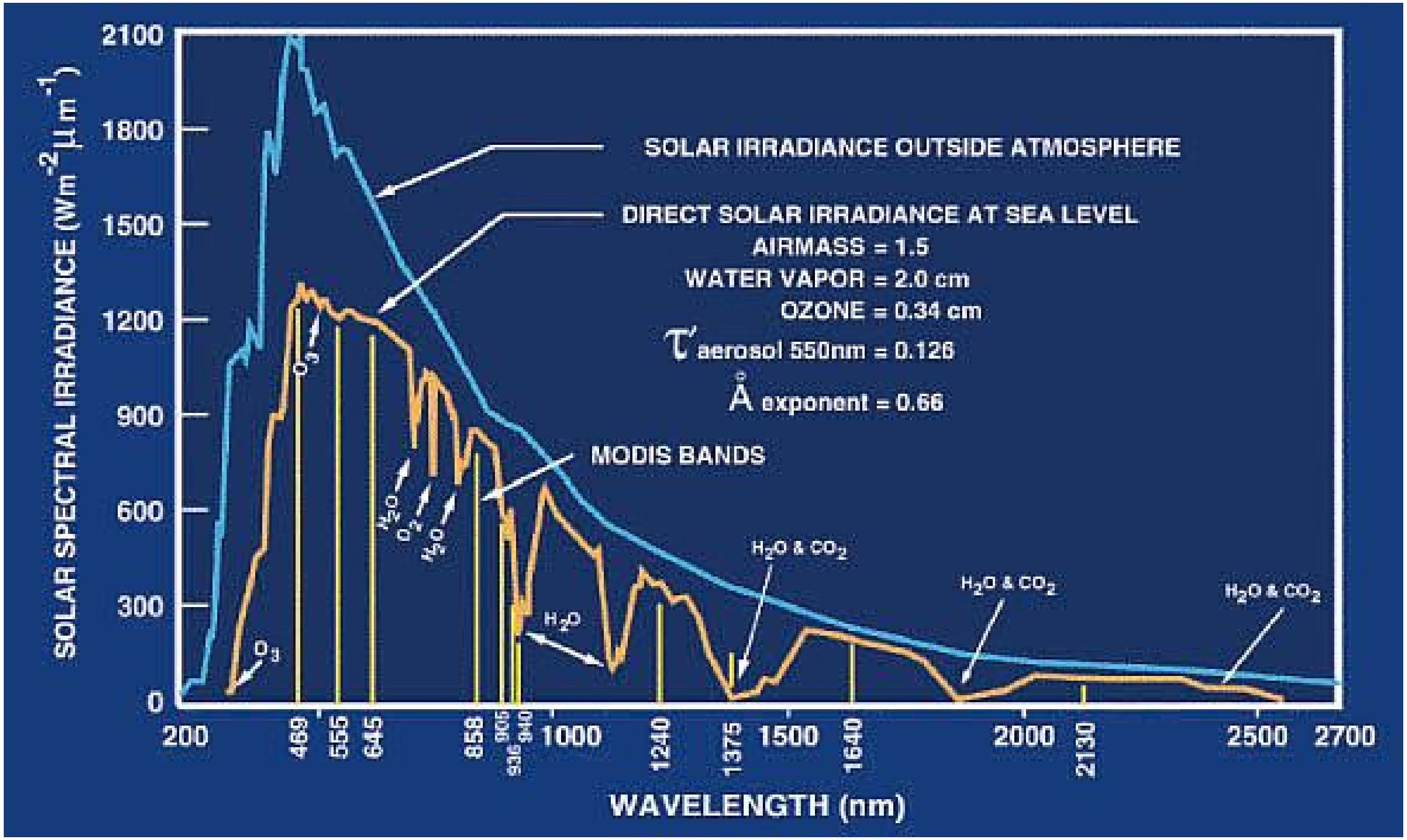

Data from MODIS (http://edcdaac.usgs.gov/modis/dataproducts.asp)

The solar constant

Most of the radiation reaching the earth stems from the photosphere. The effective temperature and effective radius of the photosphere are $T_o = 5800$ K and $r_o = 6.96 \cdot 10^8$ m, respectively. Assuming that the photosphere emits as a blackbody, the radiation flux at its outer limit can be computed according to Stefan-Boltzmann's law as:

$$F_o = \sigma T_o^4$$

where

$\sigma = 5.67 \cdot 10^{-8}$ W m^{-2} K^{-4}, Stefan-Boltzmann constant.

Since the propagating solar radiation has a spherical wavefront, at a distance d from the sun's center the flux of solar radiation has decreased to:

$$F(d) = F_o \frac{4\pi r_o^2}{4\pi d^2} = F_o \left(\frac{r_o}{d} \right)^2$$

The solar constant (2)

The <u>solar constant</u> $S_o \equiv F(a)$ is defined as the flux of solar radiation at the top of the atmosphere (TOA) at the mean distance a between the earth and the sun. The earth's orbit being an ellipse, the mean distance is equal to the major semiaxis, $a = 1.496 \cdot 10^{11}$ m, giving $S_o = 1367$ W m^{-2}.

Knowledge of the astronomical settings allows to compute the solar constant for all other planets, too. Values of a and S_o for the three terrestrial planets are listed in the following table. Astronomical parameters for all of the planets are provided in the table on the next page.

Planet	a [m]	S_o [W m^{-2}]
Venus	$1.082 \cdot 10^{11}$	2637
Erde	$1.496 \cdot 10^{11}$	1367
Mars	$2.279 \cdot 10^{11}$	592

Key data for the planets

4 Sonnensystem

4.1 PLANETEN

Symbol	Merkur ☿	Venus ♀	Erde ⊕	Mars ♂	Jupiter ♃	Saturn ♄	Uranus ⛢	Neptun ♆	Pluto PL	*Einheiten*
Äquatorradius										
– absolut	2.425	6.070	6.378	3.395	71.3	60.1	24.5	25.1	2.9	10^6 m
– relativ	0.380	0.952	1.000	0.532	11.18	9.42	3.84	3.93	0.46	$R_\oplus$
Große Bahnhalbachse										
– absolut	57.9	108.2	149.6	227.9	778.3	1427.0	2869.6	4496.6	5900	10^9 m
– relativ	0.387099	0.723332	1.000000	1.523691	5.202803	9.53884	19.1819	30.0578	39.44	AE
Mittlerer, scheinbarer «Oppositions»-Durchmesser	10.9″	61.0″		17.9″	46.9″	19.5″	3.6″	2.1″	0.22″	
Numerische Bahnexzentrizität	0.205628	0.006787	0.016722	0.093377	0.04845	0.05565	0.04724	0.00858	0.250	
Bahnneigung gegen Ekliptik	7°00′15″	3°23′40″		1°51′00″	1°18′17″	2°29′22″	0°46′23″	1°46′22″	17°10′	
Siderische Umlaufszeit	87.969	224.701	365.256	686.980	4332.589	10 759.22	30 685.4	60 189	90 465	d
Siderische Umlaufszeit	0.24085	0.61521	1.00004	1.88089	11.86223	29.4577	84.0139	164.793	247.7	a
Mittl. Bahngeschwindigkeit	47.89	35.03	29.79	24.13	13.06	9.64	6.81	5.43	4.74	km/s
Synodische Umlaufszeit	115.88	583.92		779.94	398.88	378.09	369.66	367.49	366.73	d
Siderische Rotationsdauer am Äquator (r = rückläufig)	59 d	244.3 d (r)	23.9345 h	24.6229 h	9.842 h	10.233 h	10.817 h (r)	15.80 h	6.387 d	
Neigungswinkel des Äquators zur Umlaufbahn	28°	3°	23°27′	23°59′	3°05′	26°44′	82°05′	28°48′	50° (?)	

After: DMK/DPK, 1984: Formeln und Tafeln. Orell Füssli Verlag, Zürich.

Is the solar constant really a constant?

To answer this question let us have a look at measurements of the solar constant carried out during the last 3 decades with the help of various satellites. The compilation shown below is due to Quinn and Fröhlich (1999).

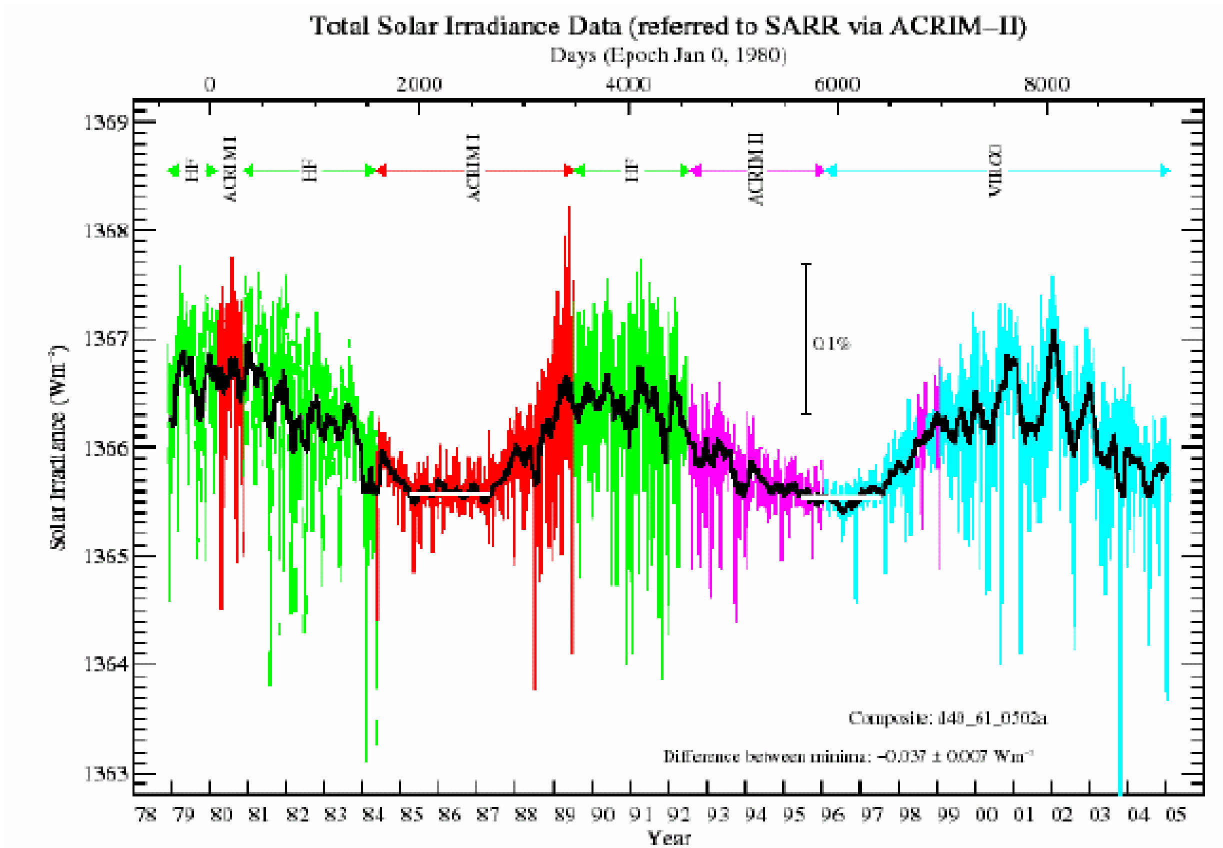

Quinn and Fröhlich (1999)

Is the solar constant really a constant? (2)

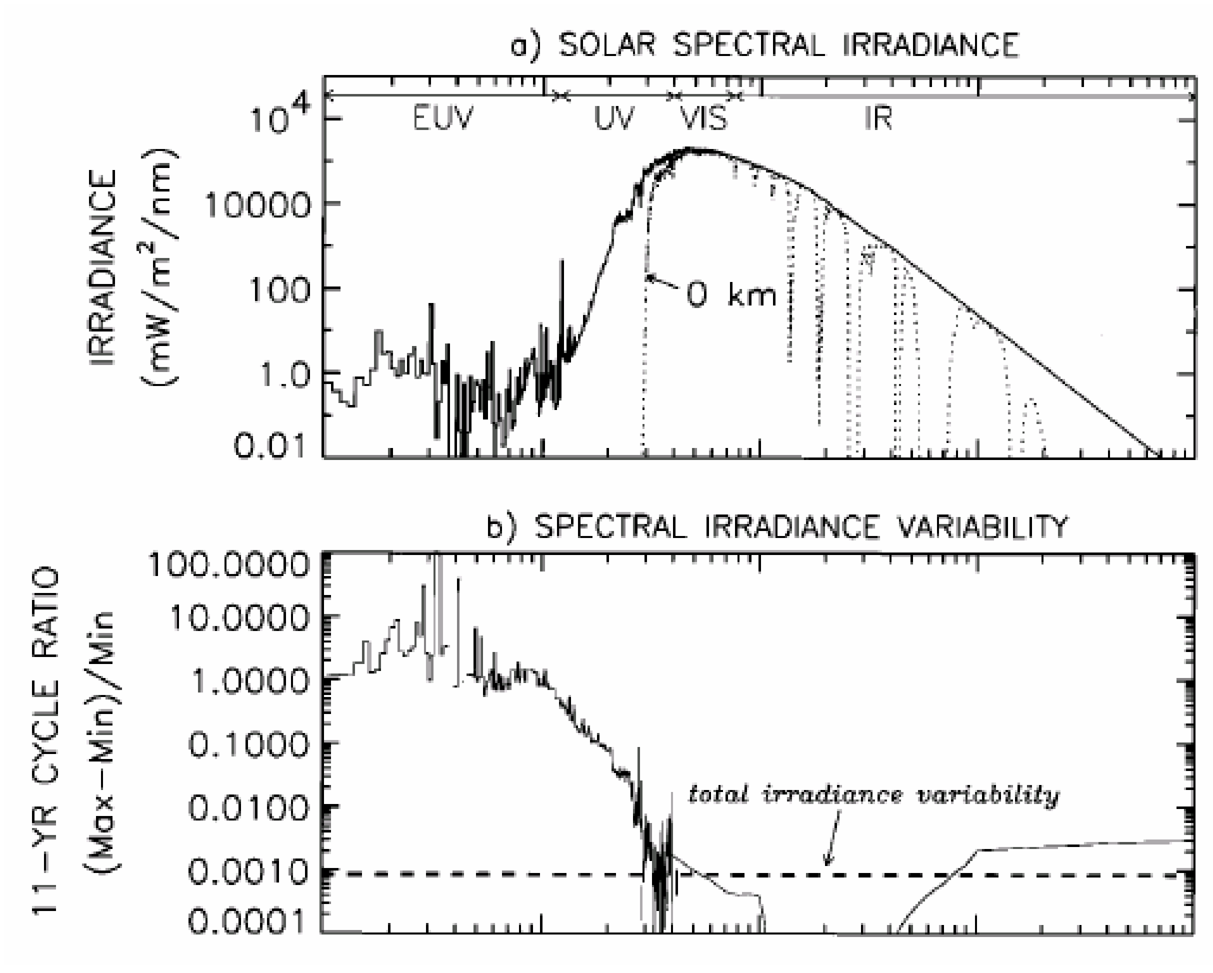

Lean and Rind (1998)

Relation between solar constant and solar activity

To explain the <u>11-years variability of the solar constant</u> it is necessary to consider the 11-years cycle of the solar activity. Although one would expect that the solar constant is lowest during periods of intense activity because the number of sunspots is highest, the reverse is actually true.

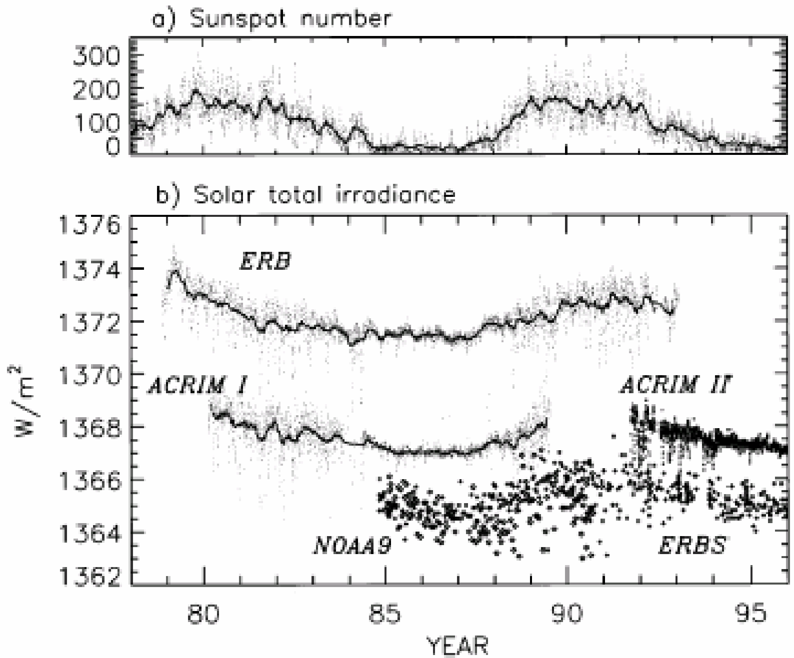

FIG. 6. Contemporary solar activity variations are indicated by the sunspot number in (a) and changes in total solar radiative output in (b), recorded by the ERB radiometer on the *Nimbus-7* satellite, ACRIM I on the *Solar Maximum Mission* (*SMM*) satellite, and ACRIM II on the *UARS*, and by the ERBE program (*NOAA-9* and *ERBS*). The solid lines in (a) and (b) are 81-day running means of the daily data, which are shown as dots. The absolute irradiance scale of the ACRIM II data has been adjusted to match that of ACRIM I using the overlapping ERBS data. Solar total irradiance increases during times of maximum solar activity (e.g., 1980 and 1990) relative to its levels in the intervening activity minimum. The differences in absolute irradiance levels among the different measurements are of instrumental origin and reflect absolute inaccuracies in the measurements. Because these inaccuracies exceed the solar cycle amplitude, the cross-calibration of successive radiometers is mandatory to preserve the historical irradiance database.

Lean, J. und D. Rind, 1998: Climate forcing by changing solar radiation. J. *Climate*, **11**, 3096-3094

Relation between solar constant and solar activity (2)

The reason is that the brightening caused by the enhanced number of faculae more than compensate for the darkening caused by the enhanced number of sunspots.

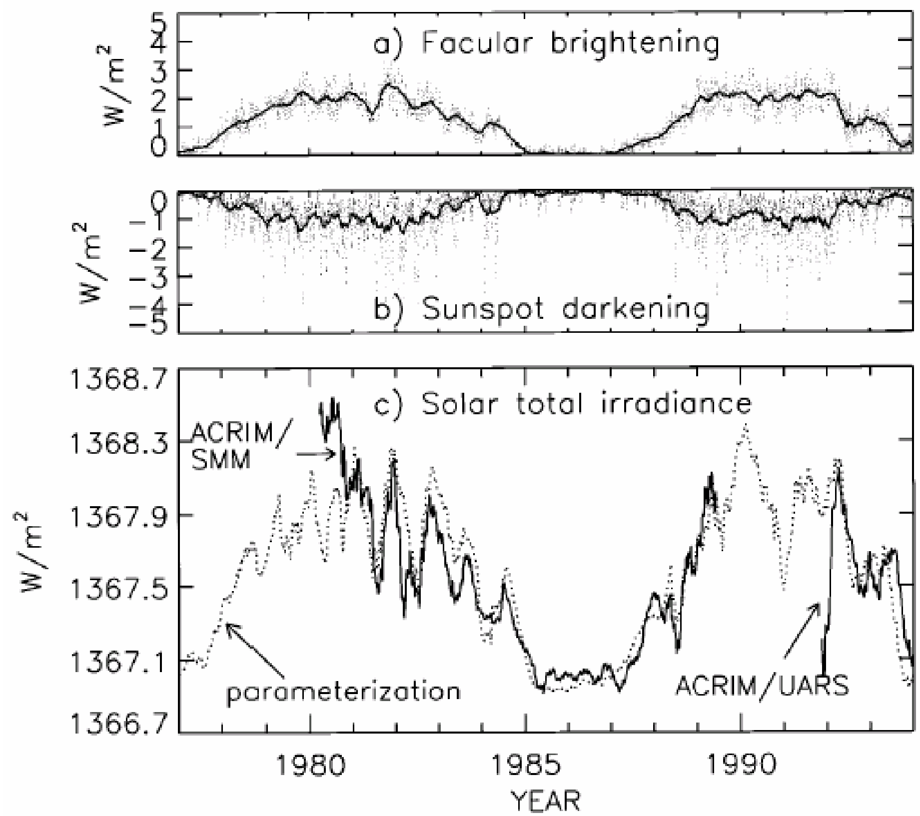

Lean, J. und D. Rind, 1998: Climate forcing by changing solar radiation. *J. Climate*, **11**, 3096-3094

The solar constant, 1600 to present

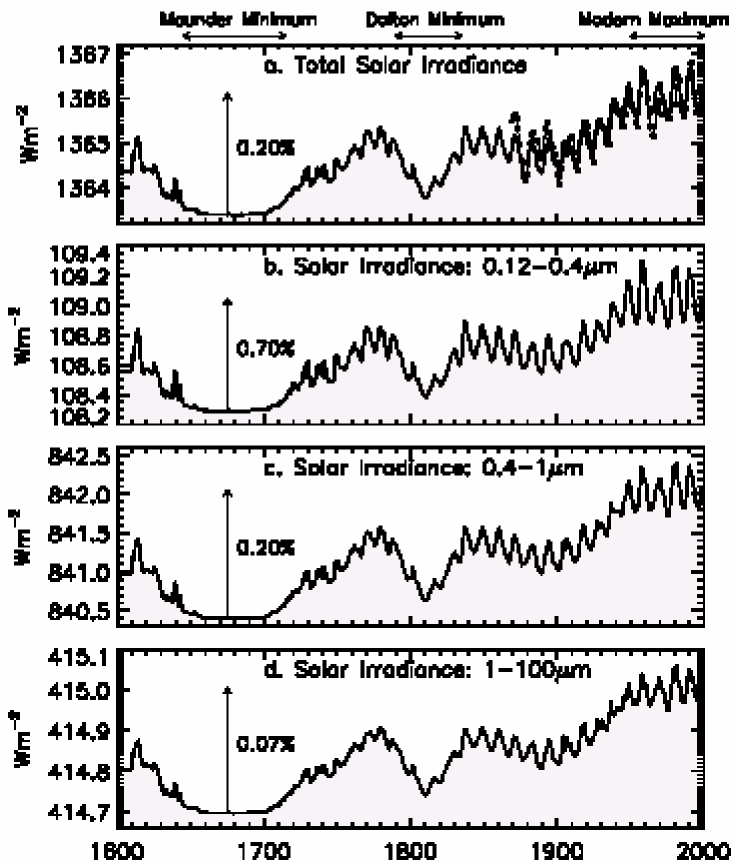

Figure 4. Compared are reconstructions of annual total irradiance in a) with spectral irradiance in broad bands from b) 0.12-0.4 μm, c) 0.4-1 μm and d) 1-100 μm. The summed bands in b), c) and d) equal the total irradiance variations in a). The shading identifies 11-year running means and the arrows show percentage increases from 1675 to the mean of cycle 22 (1986-1996). The symbols in a) are estimates of total irradiance (scaled by 0.999) determined independently by *Lockwood and Stamper* [1999].

The solar constant varies also on a <u>multi-decadal time scale</u>. These variations are of less than ~ 2 parts in 1400, that is of less than 2 ‰.

Lean, J., 2000: Evolution of the Sun's Spectral Irradiance Since the Maunder Minimum. *Geophysical Res. Letters*, **27**, 2425-2428

Decadal to centennial variability of the solar output and climate

Many researchers have postulated a correlation between the decadal variability of the solar output and various climatic parameters. A good survey is provided in the books by Hoyt and Schatten (1993) and Burroughs (2003).

A physical explanation for the observed correlations has yet to be found, and the foundation of such statistical analyses is to be considered tenuous (a statistical correlation does not necessarily imply a physical linkage!).

There are, however, a few studies that merit consideration:

- Eddy (1976, 1977);
- Lean and Rind (1998);
- Labitzke and van Loon (e.g. 1997)

Hoyt, D. V., and K. H. Schatten, 1993: *The Role of the Sun in Climate Change.* Oxford University Press, 279 pp;

Burroughs, W.J., 2003: *Weather Cycles: Real or Imaginary?* Second Edition, Cambridge University Press, 317 pp;

Labitzke, K. and H. van Loon, 1997: The signal of the 11-year sunspot cycle in the upper troposphere-lower stratosphere. *Space Science Reviews*, 80, 393-410

Solar activity and winter severity

By looking at the historic record of winter severity (through analysis of proxy data) and the number of sunspot, Eddy (1976, 1977) found that during the so-called Little Ice Age the most severe winter were concomitant with periods characterized by the absence of sunsports.

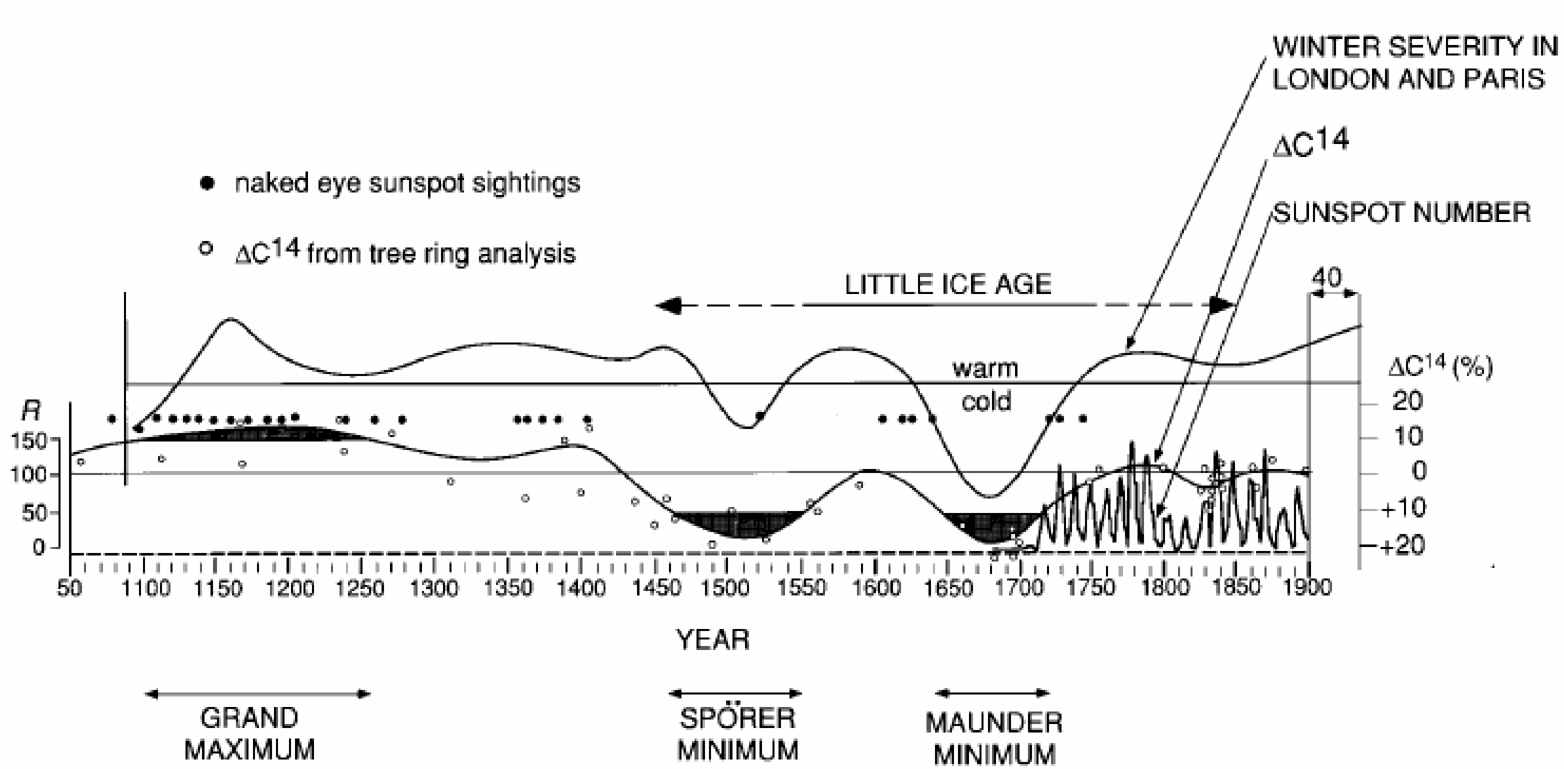

Solar activity and NH temperature

Moreover, Lean and Rind (1998) found that: ‘The correlation of reconstructed solar irradiance and Northern Hemisphere (NH) surface temperature anomalies is 0.86 in the preindustrial period from 1610 to 1800, implying a predominant solar influence. Extending this correlation to the present suggests that solar forcing may have contributed about half of the observed 0.55 C surface warming since 1900 and one-third of the warming since 1970’

.

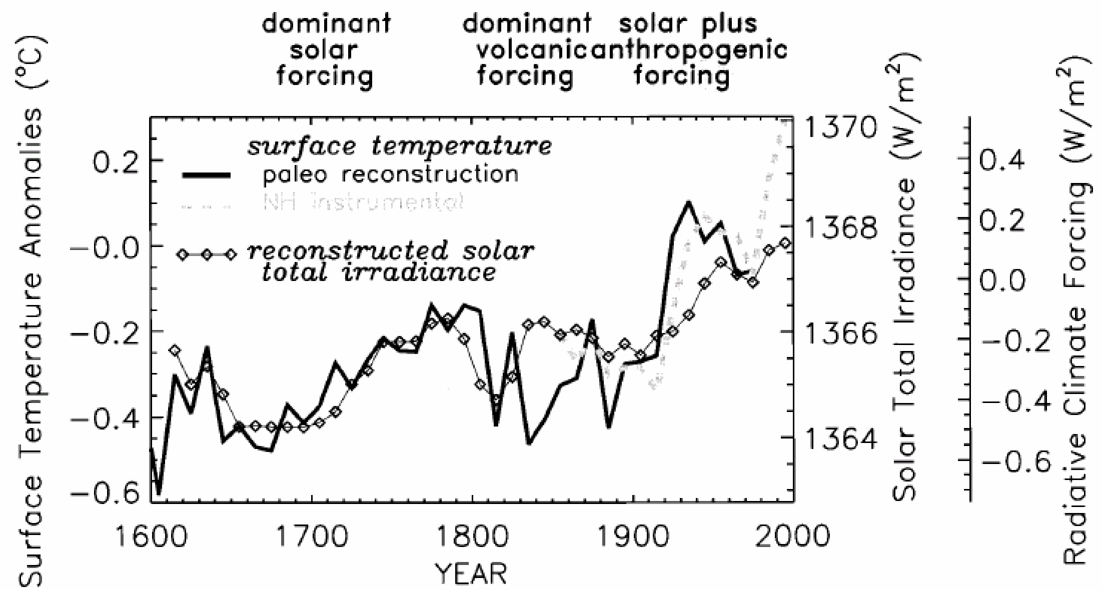

FIG. 16. Compared are decadally average values of the Lean et al. (1995b) reconstructed solar total irradiance (diamonds) from Fig. 13 and NH summer temperature anomalies from 1610 to the present (similar annually averaged data are shown in Fig. 2). The solid line is the Bradley and Jones (1993) NH summer surface temperature reconstruction from paleoclimate data (primarily tree rings), scaled to match the NH instrumental data (Houghton et al. 1992) (dashed line) during the overlap period as given in Fig. 1.

Solar activity and NH temperature (2)

Note, however, that starting about 1800 other processes appear to be significantly correlated with NH temperatures, most prominently greenhouse gases concentrations.

TABLE 3. Correlation of decadal means of solar variability, the volcanic dust veil index, and CO_2 greenhouse gas concentrations with NH surface temperature anomalies, composing the Bradley and Jones (1993) NH summer data from 1610 to 1850, scaled to Houghton et al. (1992) NH annual data, and the IPCC NH data since then, as shown in Fig. 1.

	Correlation coefficient (with NH surface temperature)	
Climate forcing parameter	1610–1800 19 points	1800–2000 20 points
Sun: reconstructed total irradiance (Lean et al. 1995b)	0.86	0.77
reconstructed total irradiance (Hoyt and Schatten 1993)	–	0.69
Volcanic dust veil index: global	−0.12	−0.57
NH	−0.005	−0.51
SH	−0.23	−0.55
Greenhouse gases: CO_2	0.70	0.86

After Lean and Rind (1998)

Note, moreover, that since relative variations in the solar constant at the decadal scale are of less than 2 ‰ (p. 8) a yet unknown amplification of the solar signal must be in place to physically explain the correlation.

.

Solar activity and the dynamics of the upper troposphere and lower stratosphere

Labitzke and van Loon (1997) have considered a possible solar signal in the height of constant-pressure levels in the upper troposphere and lower stratosphere. For the 30-hPa level the correlation is as high as ~ 0.7 in the subtropics.

.

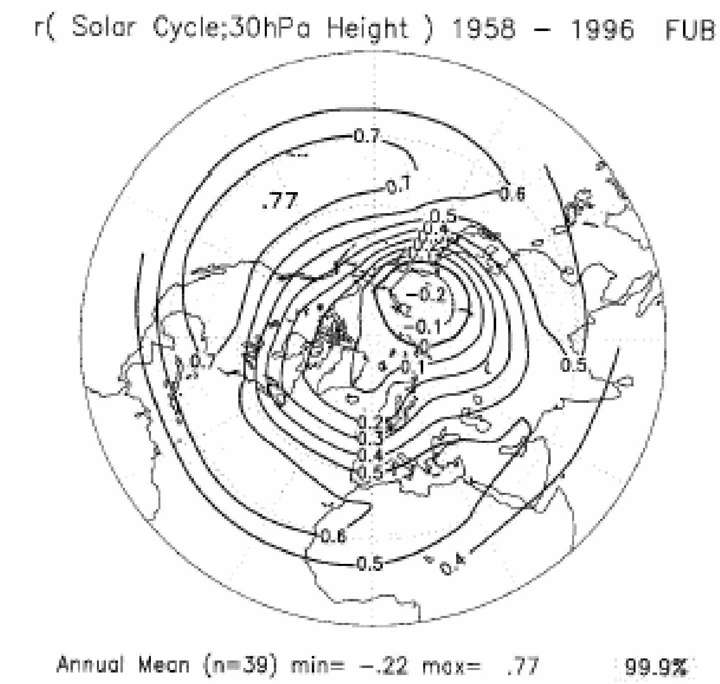

Figure 1. Correlations between the annual mean 30-hPa height and the 10.7 cm solar flux, 1958–1996.

Labitzke, K. and H. van Loon, 1997: The signal of the 11-year sunspot cycle in the upper troposphere-lower stratosphere. *Space Science Reviews*, 80, 393-410

Solar activity and the dynamics of the upper troposphere and lower stratosphere (add.)

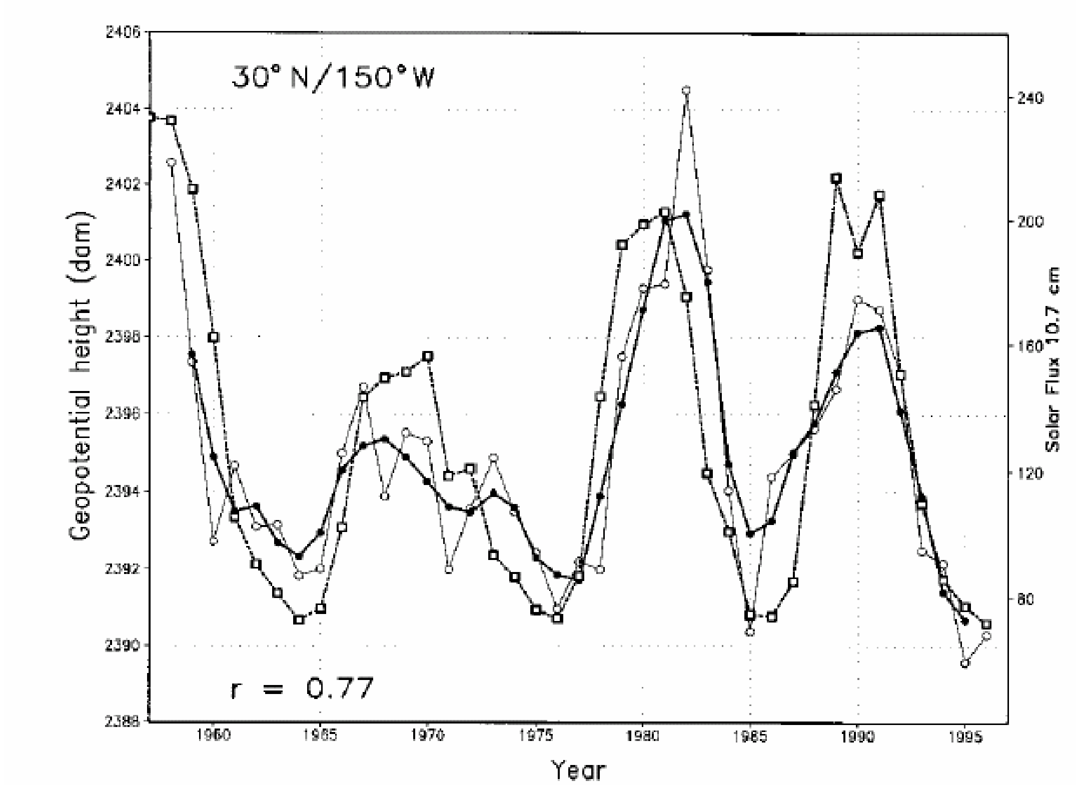

Figure 4. Time series of the 10.7 cm solar flux (dotted line), the annual mean 30-hPa height at 30° N 150° W, in geopotential dekameters (gpdam, thin solid line), and of the three-year running means of the latter curve (heavy solid line). From Labitzke and van Loon (1995) updated.

Solar activity and the dynamics of the upper troposphere and lower stratosphere (add.)

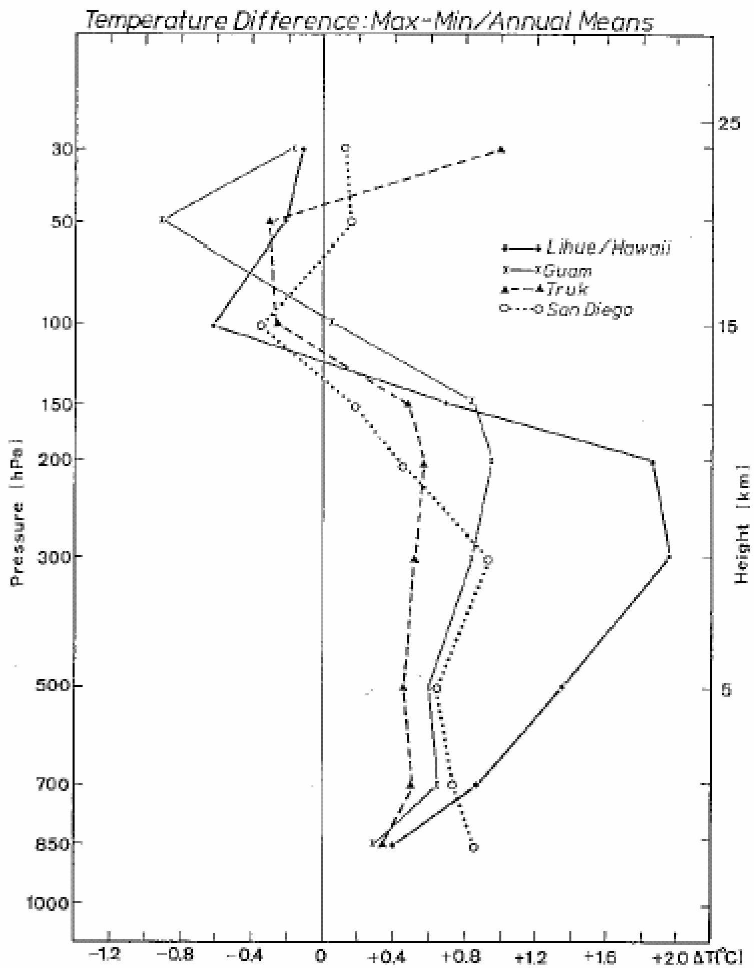

Figure 6. The annual mean temperature difference (°C) between maxima and minima in the 11-year sunspot cycle at San Diego (33° N 117°)W, Lihue (22° N 159° W), Guam (14° N 145°E), and Truk (8° N 152°E). From Labitzke and van Loon (1995), modified.

Solar activity and the dynamics of the upper troposphere and lower stratosphere (2)

For the winter season a significant correlation appears when time series are divided according to the phase of the Quasi Biennal Oscillation (QBO).

.

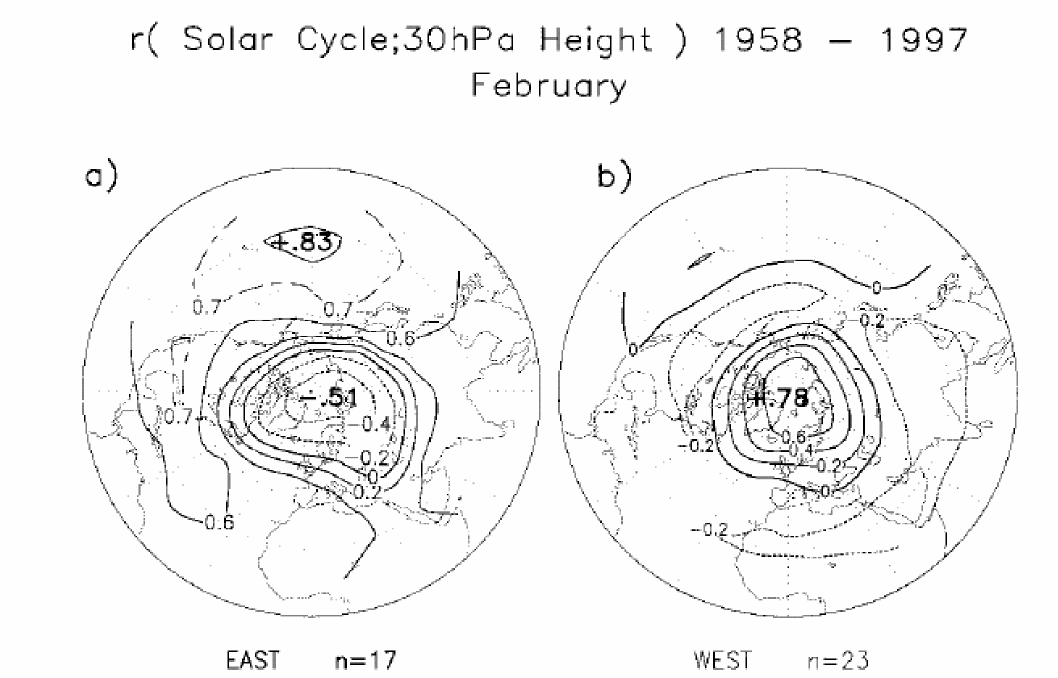

Figure 11. Correlation between the 10.7 cm solar flux and the 30-hPa height in February in (a) the east years and (b) west years of the QBO, using the average wind in January-February at the 40–50hPa levels on the equator to define the QBO.

Labitzke, K. and H. van Loon, 1997: The signal of the 11-year sunspot cycle in the upper troposphere-lower stratosphere. *Space Science Reviews*, 80, 393-410

The Quasi Biennal Oscillation

The Quasi Biennal Oscillation (QBO) (Andrews et al., 1987) is the alternation of easterly and westerly winds in the stratosphere in the layer between ~ 100 and 10 hPa.

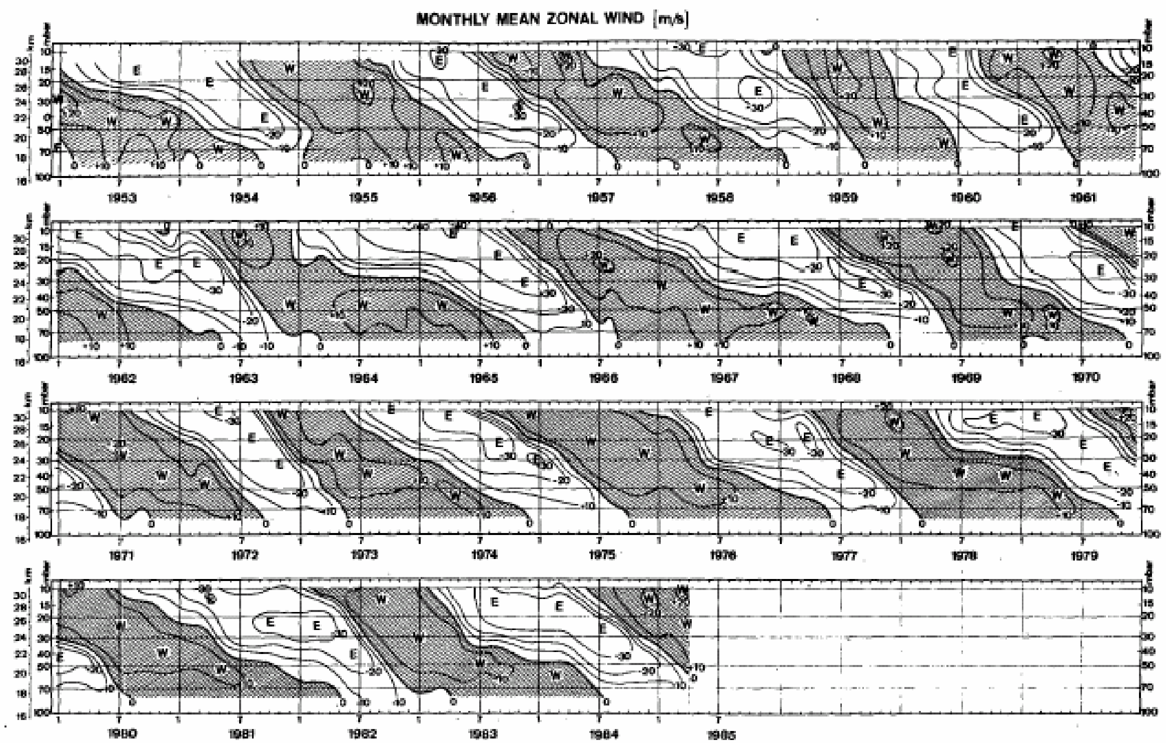

FIG. 1. Time–height section of the monthly mean zonal wind components (m s^{-1}) at Canton Island (Jan 1953–Aug 1967), Gan/Maledive Islands (Sep 1967–Dec 1975), and Singapore (Jan 1976–Apr 1985).

After Naujokat (1986)

Andrews, D.G., J.R. Holton and C.B. Levoy, 1987: Middle Atmosphere Dynamics. Academic Press, Orlando.

Orbital geometry

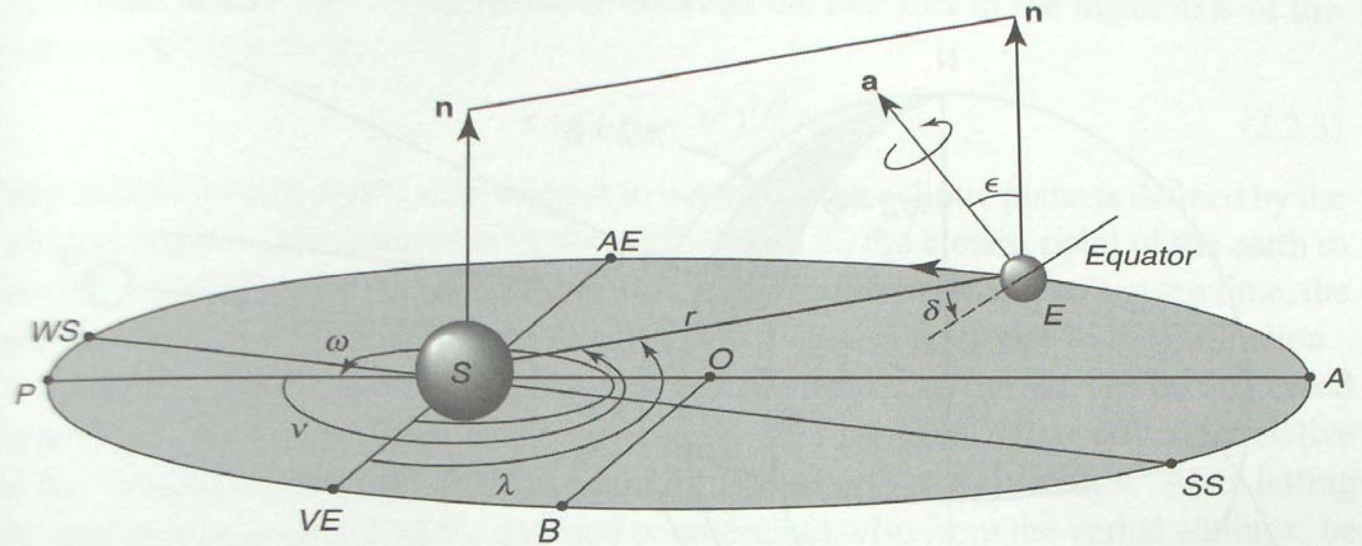

Figure 2.5 The earth–sun geometry. *P* denotes the perihelion, *A* the aphelion, *AE* the autumnal equinox, *VE* the vernal equinox, *WS* the winter solstice, and *SS* the summer solstice, **n** is normal to the ecliptic plane, **a** is parallel to the earth's axis, δ is the declination of the sun, ϵ the oblique angle of the earth's axis, ω the longitude of the perihelion relative to the vernal equinox, ν the true anomaly of the earth at a given time, λ the true longitude of the earth, *O* the center of the ellipse, *OA* (or $OP = a$) the semimajor axis, *OB* ($= b$) the semiminor axis, *S* the position of the sun, *E* the position of the earth, and *ES* ($= r$) the distance between the earth and the sun.

After Liou (2002)

Key elements of the orbital geometry

The three key elements in the orbital geometry are:

- the eccentricity, e;
- the obliquity of the earth's rotation axis relativ to the ecliptic plane, ε;
- the longitude of the perihelion, ω.

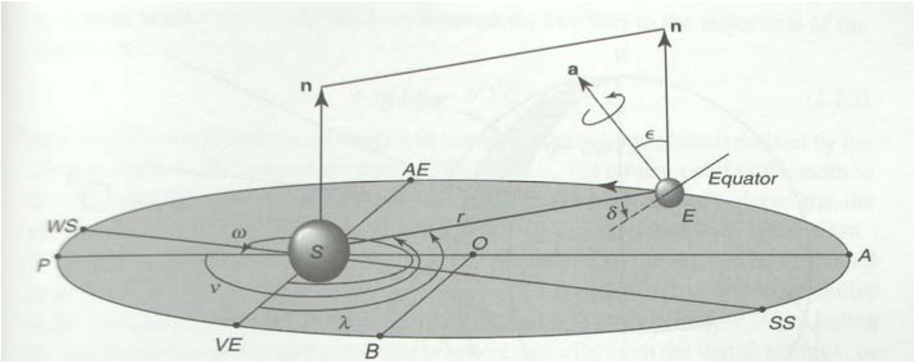

After Liou (2002)

The secular variations of the orbital elements can be computed based on celestial mechanics and are associated with the perturbations that other planets exert on earth's orbit. According to Milankovitch (1941) theory, these variations are directly or indirectly responsible for the ice-ages.

Secular variations of the orbital elements

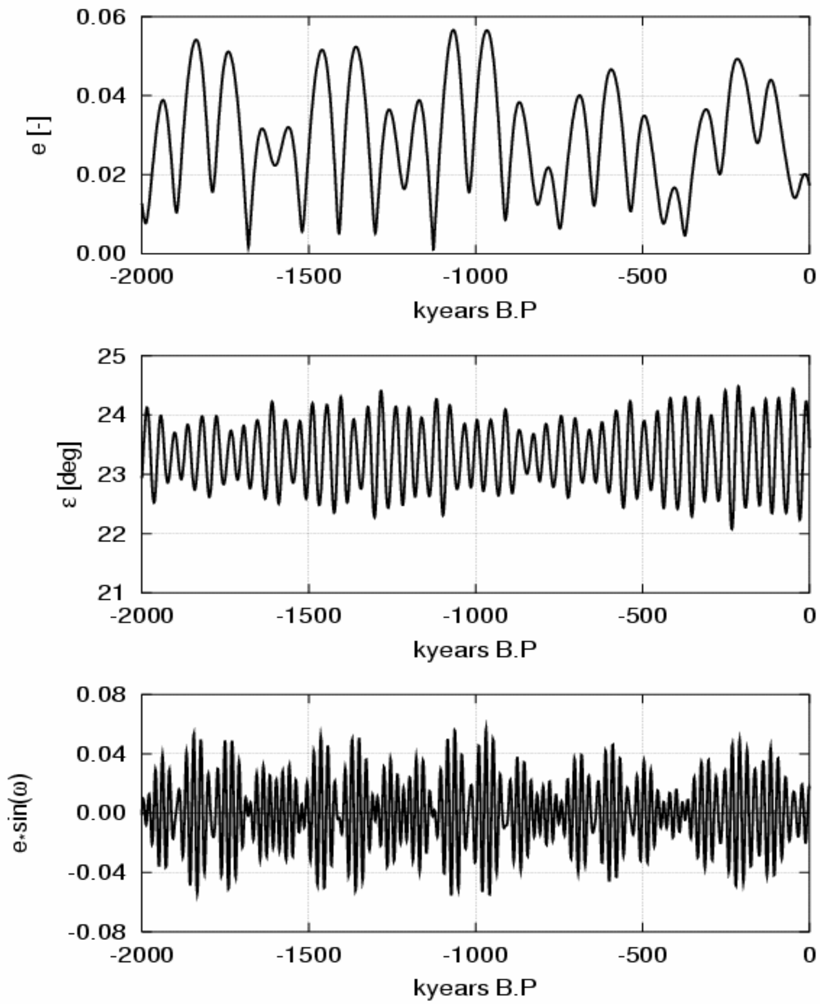

eccentricity
P of 100 and 413 kyr

obliquity
P of 41 kyr

precession, e·sin(ω),
P of 23 and 18 kyr

Data calculated according to
Berger A. and Loutre M.F., 1991: Insolation values for the climate of the last 10 million years. Quaternary Sciences Review, Vol. 10 No. 4, pp. 297-317, 1991.

Solar zenith angle

Essentially the position of the sun with respect to an observer at the surface is determined by the solar zenith angle θ_o, that is the angle between the vertical above the observer (the normal) and the sun. The solar zenith angle can be expressed in terms of the solar declination δ (the angle subtended by the sun with respect to the equatorial plane), the hour angle ω (< 0 before true solar noon, = 0 at noon, > 0 after solar noon), and the geographic latitude φ of the observer O.

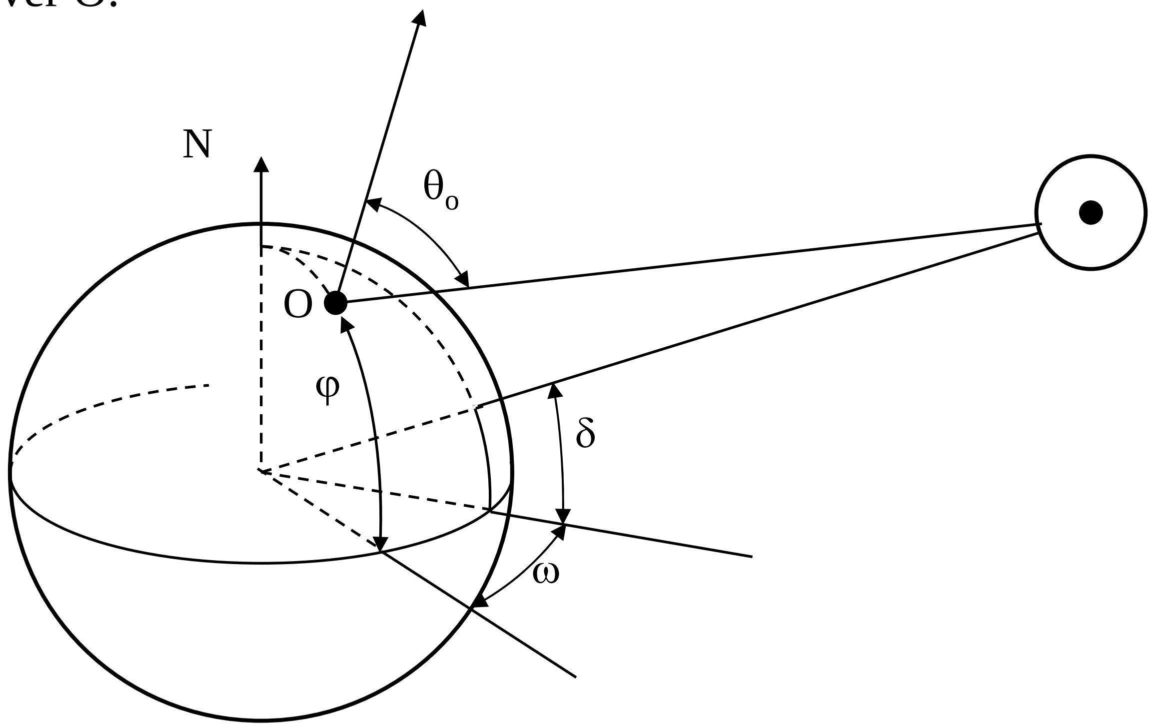

Solar zenith angle (2)

The equation reads:

$$\cos\theta_o = \sin\varphi\sin\delta + \cos\varphi\cos\delta\cos\omega$$

The hour angle is equal to zero at true solar noon, increasing by 0.26 radians or 15° pro hour. Therefore $\omega = -\pi/2$ at 6:00 and $\omega = \pi/2$ at 18:00.

Since $\theta_o = \pi/2$ at sunrise and sunset (except at the Poles), the hour angles $-\Omega$ at sunrise and Ω at sunset (atronomical values) can be found from:

$$\cos\Omega = -\tan\varphi\tan\delta$$

provided that $-1 \leq \cos\Omega \leq +1$. If $\cos\Omega > +1$ we have polar night, and if $\cos\Omega < -1$ polar day with midnight sun.

According to Iqbal (1983) a useful formula to express solar declination as a function of the running date (day of the year, $D \in [1,365]$) is:

$$\delta = 0.4093 \cdot \sin\left(\frac{2\pi}{365}D - 1.3944\right) \qquad \text{[radians]}$$

Iqbal, M. 1983: *An Introduction to Solar Radiation*. Academic Press, Toronto, 390 pp

Solar path

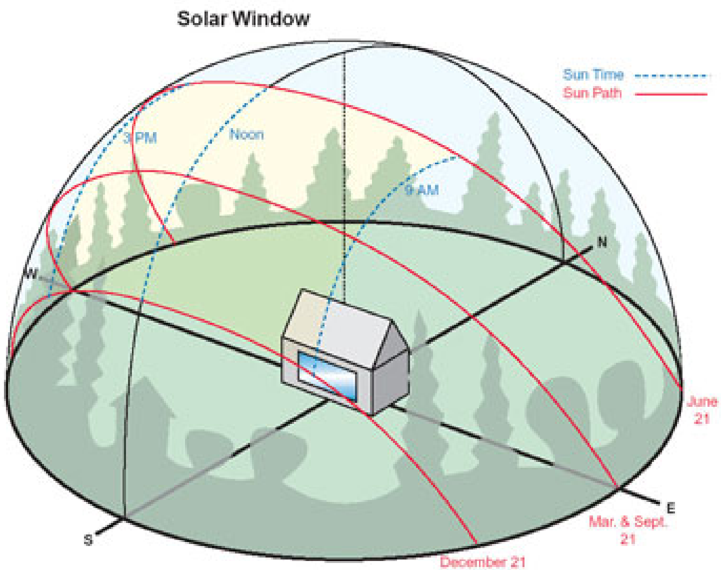

Source:
http://www.oksolar.com/abctech/solar-radiation.htm

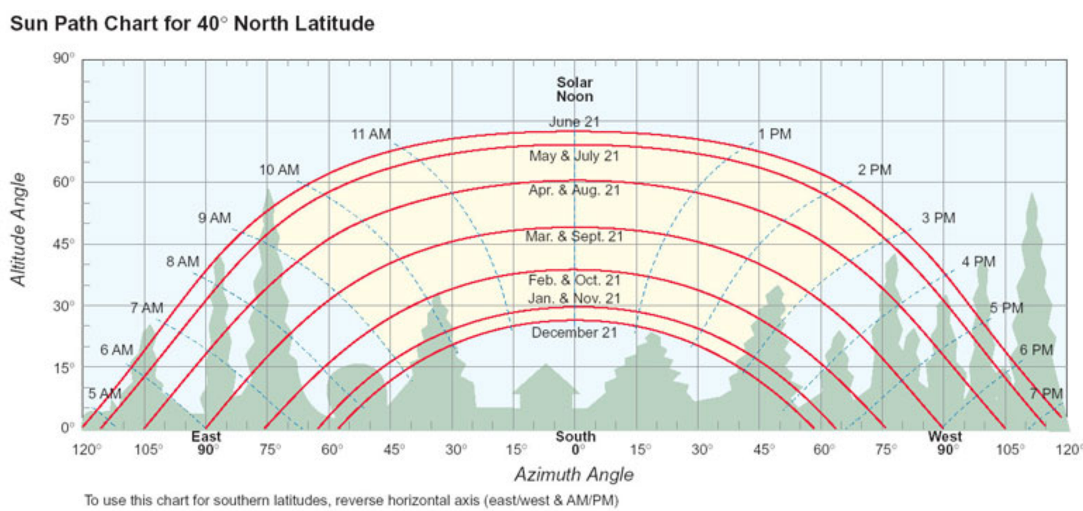

Calanca, 02.05.2006

Solar insolation at TOA

The distribution of solar insolation at the top of the atmosphere is given by:

$$S = S_o \left(\frac{a}{r}\right)^2 \cos\theta_o$$

where S_o is the solar constant, a the mean distance between the sun and the earth, and r the current distance at a particular day of the year D. Following Iqbal (1983), the square of the ratio (a/r) can be calculated as:

$$\left(\frac{a}{r}\right)^2 = 1 + 0.033 \cdot \cos\left(\frac{2\pi}{365} D\right)$$

Note: more accurate formulas for the solar declination and the relative distance to the sun can be found in Iqbal (1983) or Liou (2002).

The daily insolation is found by integrating the above equation between sunrise and sunset:

$$S_D = \int_{-\Omega}^{\Omega} S_o \left(\frac{a}{r}\right)^2 \sin\delta \sin\varphi + \cos\delta \cos\varphi \cos\omega \, d\omega$$

$$= 2 S_o \left(\frac{a}{r}\right)^2 \left[\Omega \sin\delta \sin\varphi + \cos\delta \cos\varphi \sin\Omega\right]$$

Distribution of daily insolation at TOA

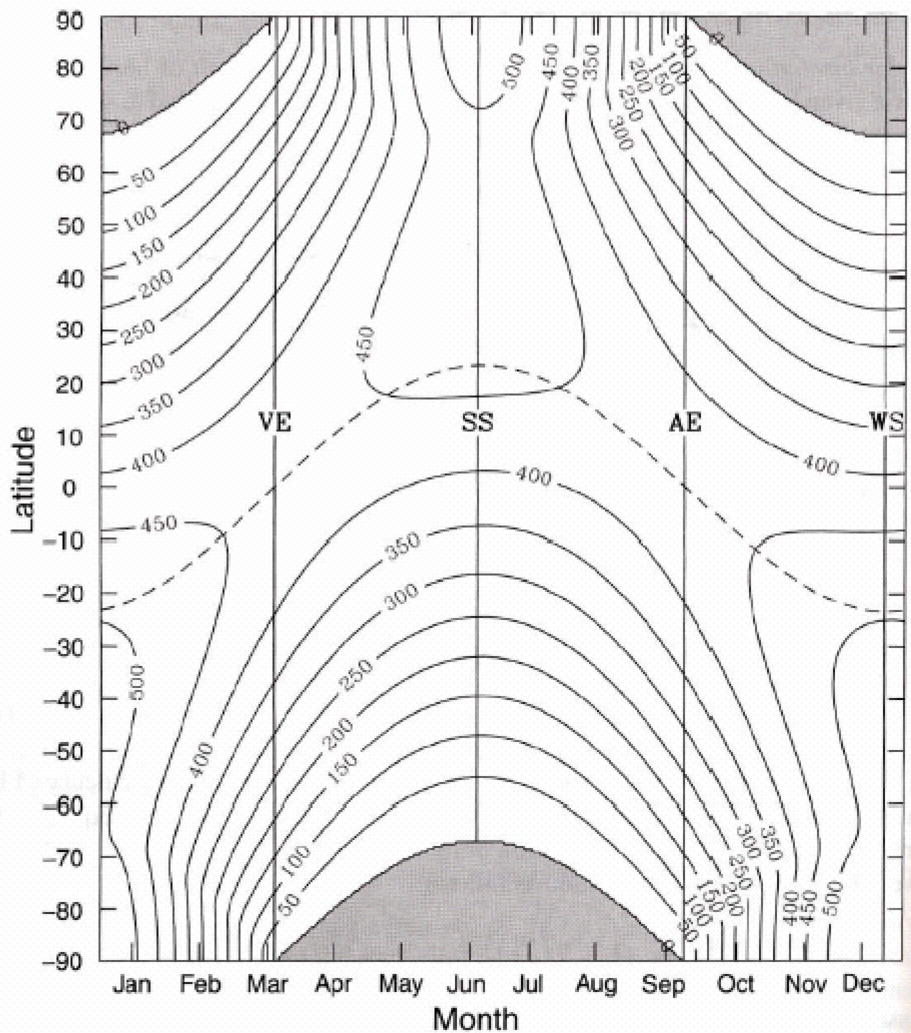

Figure 2.8 Daily mean solar insolation (Q/24 hr) as a function of latitude and day of year in units of W m^{-2} based on a solar constant of 1366 W m^{-2}. The shaded areas denote zero insolation. The position of vernal equinox (VE), summer solstice (SS), autumnal equinox (AE), and winter solstice (WS) are indicated with solid vertical lines. Solar declination is shown with a dashed line.

After Liou (2002).

Annual mean insolation at TOA

The annual mean insolation $\langle S \rangle$ can be evaluated via Kepler's second law. The calculation are too lengthy to be reported here, but can be found in the notes of the course 'Theoretical Climatology'.

The final result is:

$$\langle S \rangle = \frac{S_o}{4\sqrt{1-e^2}} \cong \frac{S_o}{4}$$

where e is the eccentricity of the earth orbit. It is defined as the ratio between the two foci and the major axis:

$$e = \frac{\left(a^2 - b^2\right)^{1/2}}{a}$$

(b is the minor axis) and is currently equal to 0.016722.

Annual mean insolation at TOA

As for the latitudinal distribution of the annual mean insolation we have:

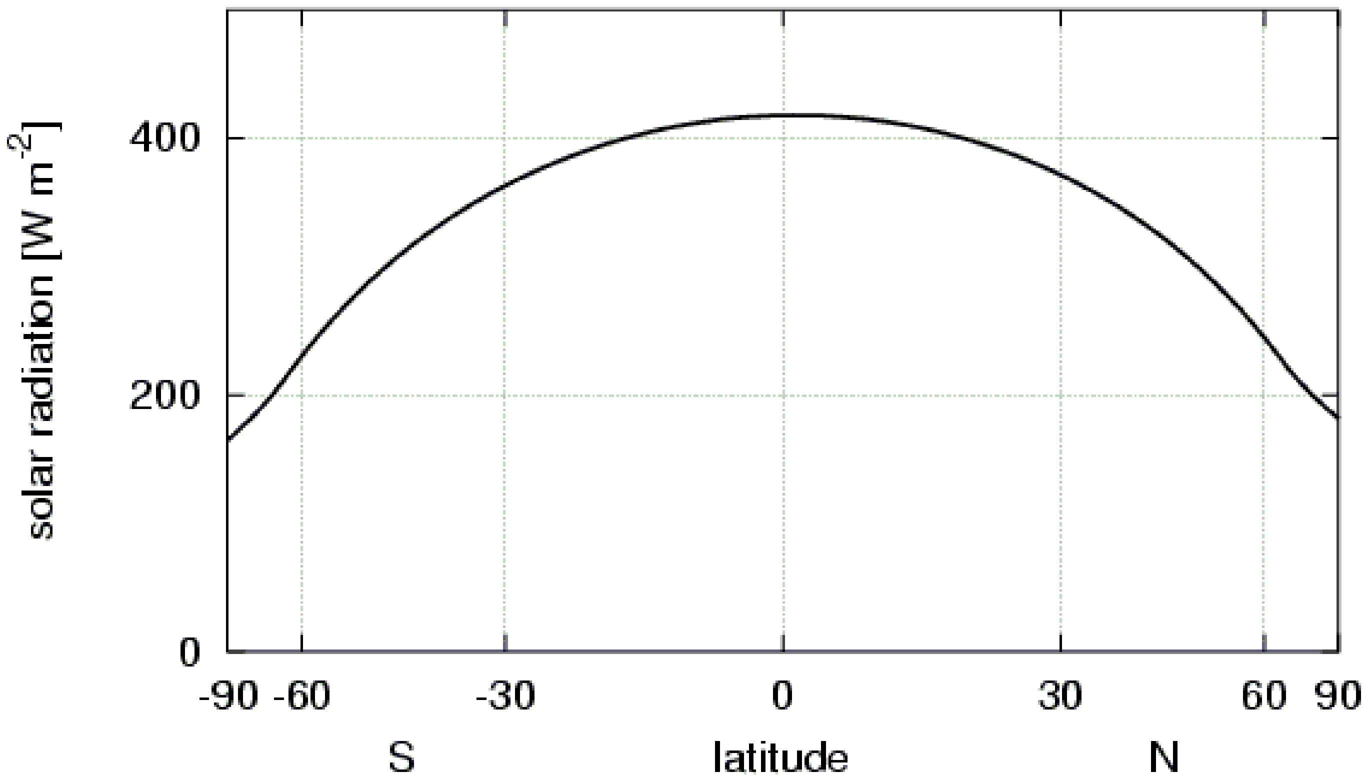

Zenith angle and air mass

When considering absorption and scattering of solar radiation it is necessary to know the total mass of absorbing or scattering substance. Recall the Beer-Bouguer-Lambert law:

$$N_\lambda(s) = N_{\lambda 0}\exp\left(-k_\lambda \int_0^s \rho\, ds\right) \equiv N_{\lambda 0}\exp(-k_\lambda u)$$

where us is the optical path. The distance covered by a beam in the atmosphere depends on the solar zenith angle:

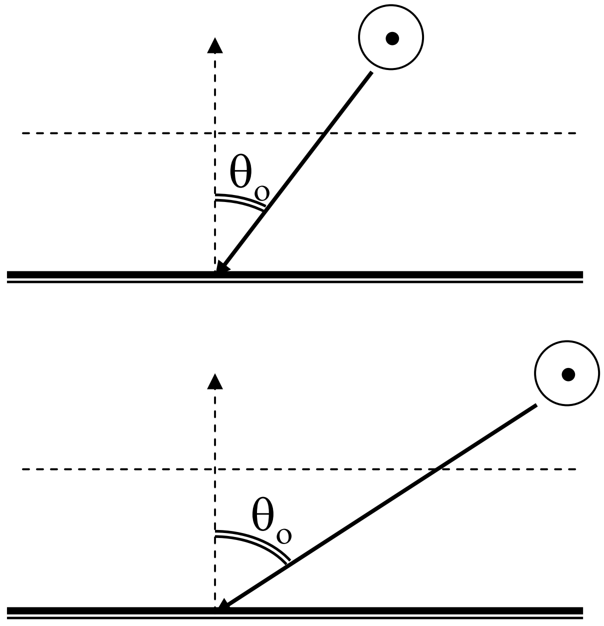

Zenith angle and air mass (2)

To account for the effect of the zenith angle, we make use of the so-called <u>relative optical air mass</u> defined as (Paltridge and Platt, 1976):

$$m = \frac{\int_0^{\infty} \rho \, dz}{\int_0^{\infty} \rho \, ds}$$

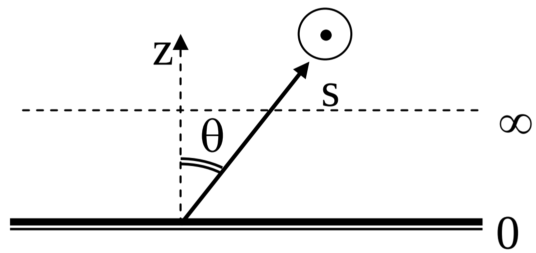

As seen in the above figure, to the extent that the atmosphere can be considered as a non-refreacting, plane-parallel medium:

$$m = \frac{1}{\cos \theta_o} \equiv \sec \theta_o$$

In practice, due to the curvature of the earth's atmosphere and the density dependence of the refractive index, this equation holds true only for $\theta_o < 60^o$. A more accurate formula is due to Kasten (1966). It reads:

$$m = \left\{ \sin \gamma_o + 0.15 \cdot (\gamma_o + 3.885)^{-1.253} \right\}^{-1}$$

where $\gamma_o = 90^o - \theta_o$ is the observed solar altitude (in degrees).

Radiation at ground: direct and indirect irradiance

Atmospheric scatter ensures that the downcoming flux density has a direct as well as a diffuse component. At any solar zenith angle θ_o the total vertical flux density, the so-called global radiation, is given by (Paltridge and Platt, 1976):

$$Gl \equiv F\downarrow = F_{dir} \cos\theta_o + \int N_{diff}\, d\omega$$

where F_{dir} is the irradiance of the direct beam on a surface perpendicular to the beam abd N_{diff} is the radiance of diffuse radiation and the integral is over the all solid angles of the upper hemisphere.

In terms of the total optical depth $[(\tau_{R,\lambda} + \tau_{oz,\lambda} + \tau_{wv,\lambda} + \tau_{D,\lambda})\, m]$ realtive to the extinction of solar radiation by Rayleigh scattering, ozone and water vapor absorption and extinction by aerosols, the direct beam can be expressed as:

$$F_{dir} = \int_0^\infty S_\lambda \exp\left[-\left(\tau_{R,\lambda} + \tau_{oz,\lambda} + \tau_{wv,\lambda} + \tau_{D,\lambda}\right) m\right] d\lambda$$

where S_λ is the spectral radiance at the top of the atmosphere (see p.23).

Direct radiation

The formula for the direct radiation can be simplified by introducing the <u>transmissivity</u>, given (see class on 'Radiative Transfer') as

$$T_\lambda \equiv \exp(-\tau_\lambda)$$

which allows one to write:

$$F_{dir} = \int_0^\infty S_\lambda \left(T_{R,\lambda} \cdot T_{oz,\lambda} \cdot T_{wv,\lambda} \cdot T_{D,\lambda}\right)^m d\lambda$$

By defining the <u>transmittance</u> (transmission function) q as the 'average' transmissivity of the atmosphere, such that:

$$F_{dir} = q^m \int_0^\infty S_\lambda \, d\lambda$$

the formula for the direct radiation reduces to:

$$F_{dir} = S q^m = S_o \left(\frac{a}{r}\right)^2 q^m \cos\theta_o$$

Note that the <u>global average</u> of q for a <u>cloudless atmosphere</u> has been estimated in ~ 0.7.

Absorption of solar radiation by water vapor

According to the picture of the global energy balance presented by Kiehl and Trenberth (1997) and later published in the Third Assessment Report by the IPCC, the atmosphere absorbs in total about 67 W m^{-2}, that is 19% of the solar irradiance at the top of the atmosphere.

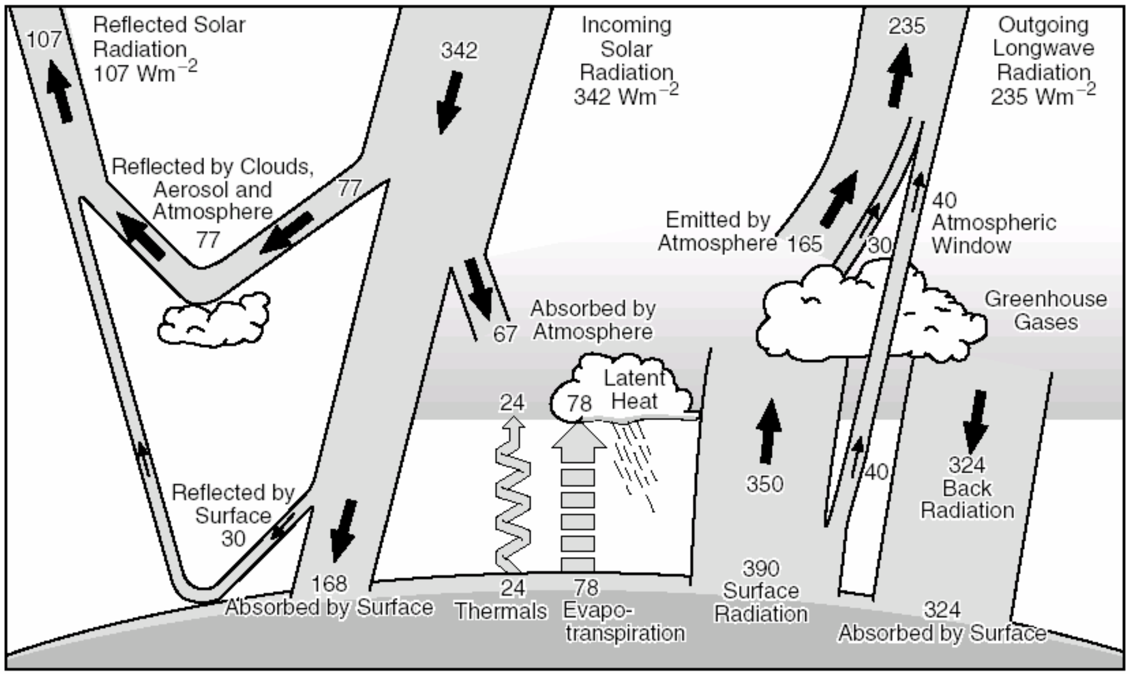

After Kiehl, J.T. and K.E. Trenberth, 1997: Earth's Annual Global Mean Energy Budget, *Bull. Am. Met. Soc.*, **78**, 197-208

Absorption of solar radiation by water vapor (2)

However, detailed calculations with MODTRAN as well as an evaluation of data from the Baseline Surface Radiation Network (Ohmura et al., 1998) suggest that the total absorption must be in the order of 28 %, with an absorption of ~ 70 W m^{-2} alone by water vapor (assuming an average total content of 25 kg m^{-2}).

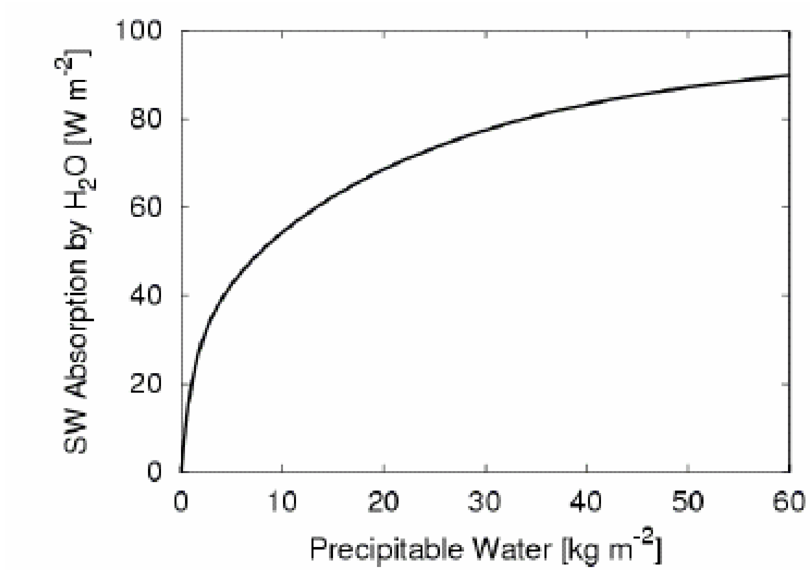

Ohmura, A., H. Gilgen, H. Hegner, G. Müller, M. Wild, E.G. Dutton, B. Forgan, C. Fröhlich, R. Philipona, A. Heimo, G. König-Langlo, B. McArthur, R. Pinker, C.H. Whitlock, and K. Dehne, 1998: Baseline Surface Radiation Network (BSRN/WCRC): new precision radiometry for climate research, *Bull. Amer. Meteor. Soc.*, 79(10), 2115-2136.

Distribution of selected fluxes of solar radiation

All of the following picture refer to annual mean fluxes and were taken from Raschke and Ohmura (2005). First we show a map of the net solar radiation at the top of the atmosphere.

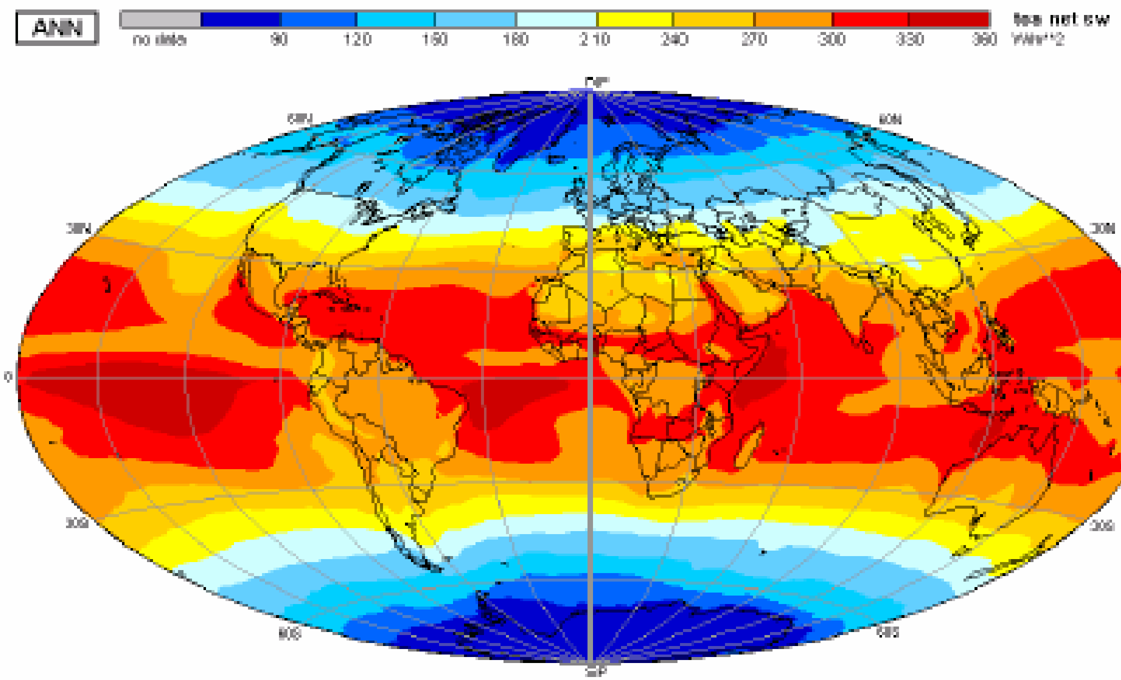

4.3.3.2a Annual averages of the solar net radiation at top of the atmosphere (or (1.0 − albedo) × incident radiation) **in Wm^{-2}** of the period 1991 to 1995. This quantity is equivalent to the amount of solar radiation absorbed in the earth-atmosphere system. Due to the low surface albedo and the relatively small cloudiness, the subtropical ocean areas gain highest amounts of solar energy. Highest and lowest values are 352 and 56 Wm^{-2} ; global average: 236 Wm^{-2}.

Raschke, E. and A. Ohmura, 2005: Radiation budget of the climate system. In Hantel (ed.), Landolt-Börnstein, Group V, Vol. 6, Observed Global Climate, Springer, Berlin.

Distribution of the selected fluxes of solar radiation (2)

Map of the global radiation at the earth's surface.

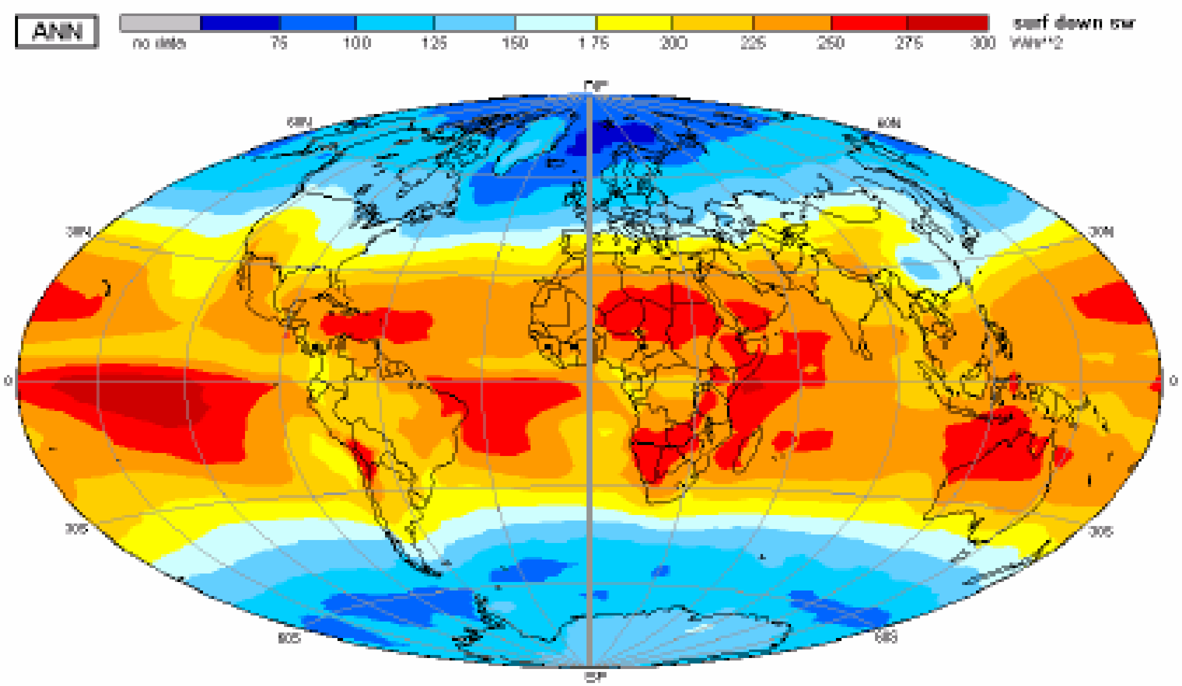

Fig. 4.3.4.3a Annual average of the downward solar radiation at ground during the period 1991 to 1995 in Wm^{-2}. Prime modifiers of these fields are the mean solar height over each area and the persistence and thickness of cloud fields. Note the low amounts over southern China. Extreme small values are obtained over the northernmost Atlantic Ocean. Highest and lowest values: 286 and 60 Wm^{-2}; global average: 189 Wm^{-2}. The values are possibly too high by about 5 to 10 Wm^{-2} as preliminary comparisons with ground-based measurements have shown.

Raschke, E. and A. Ohmura, 2005: Radiation budget of the climate system. In Hantel (ed.), Landolt-Börnstein, Group V, Vol. 6, Observed Global Climate, Springer, Berlin.

Distribution of the selected fluxes of solar radiation (3)

Map of the mean transmittance.

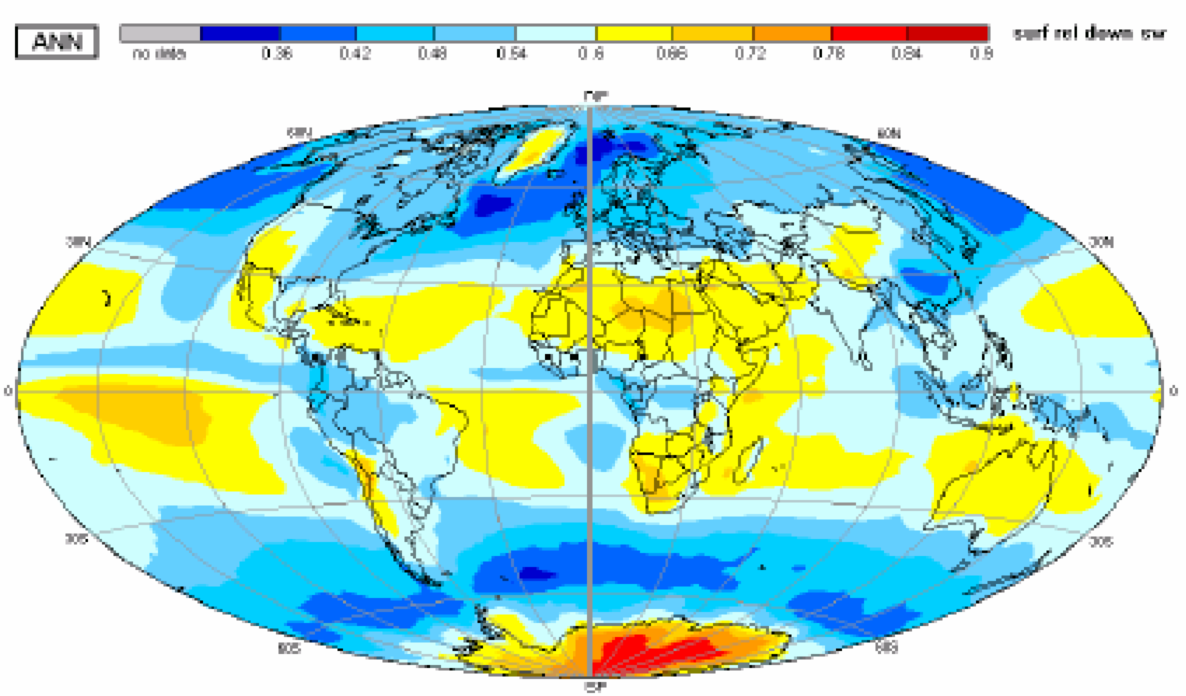

Fig. 4.3.4.3b Annual average of the relative values of the downward solar radiation at ground, related to the incident radiation at the top of the atmosphere during the period 1991 to 1995. These values are equivalent to a mean atmospheric transmittance of the atmosphere for solar radiation. This presentation enhances the role of cloud fields and of the topographic height of various continental surfaces. Highest and lowest values: 0.82 and 0.33; global average: 0.55. Such relative information is very important for initial planning of environmental projects.

Raschke, E. and A. Ohmura, 2005: Radiation budget of the climate system. In Hantel (ed.), Landolt-Börnstein, Group V, Vol. 6, Observed Global Climate, Springer, Berlin.

Global radiation and atmospheric transmittance

Contrary to what expressed by Budyko in 1982, many studies carried out during the last 15 years have demonstrated that global radiation observed at the earth's surface is far from being stable on a decadal scale. From 1950 to about 1990 many stations around the world displayed a decrease in solar radiation (the so-called ‘global dimming’); in many places this has been followed by a inverse tendency (‘global brightening’) (Wild et al., 2005).

Part of these changes can be attributed to changes in cloudiness. However, part of the variations are related to changes in the transmittance of the cloudless atmosphere, which ultimately are related to changes in the aerosol load.

Wild, M., H. Gilgen, A. Roesch, A. Ohmura, C.N. Long, E.G. Dutton, B. Forgan, A. Kallis, V. Russak, A. Tsekov, 2005: From Dimming to Brightening: Decadal Changes in Solar Radiation at Earth's Surface. Science, 308, 847-850.

Global radiation and atmospheric transmittance (2)

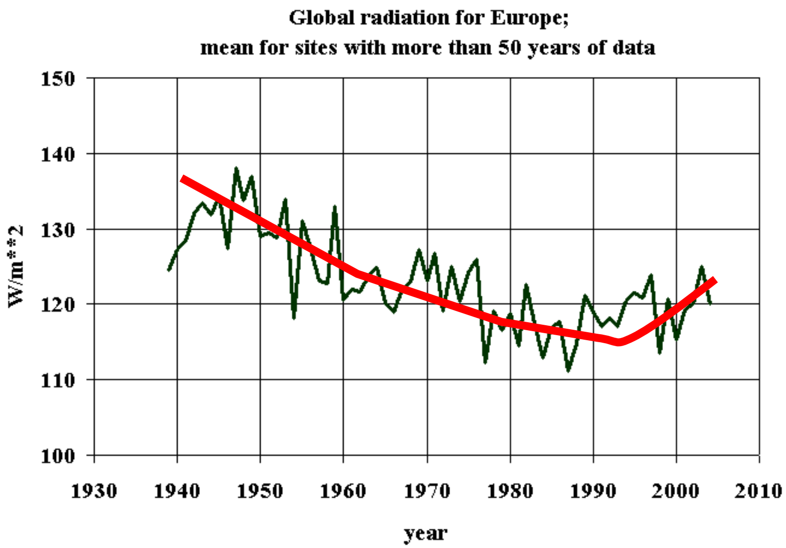

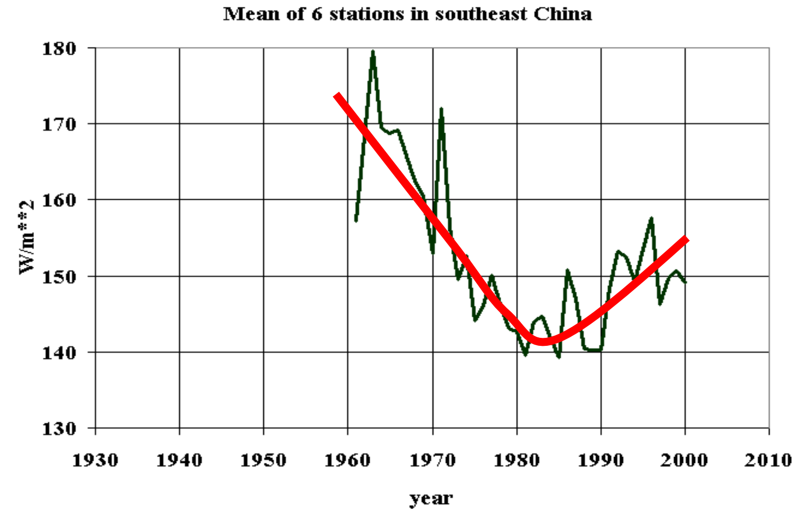

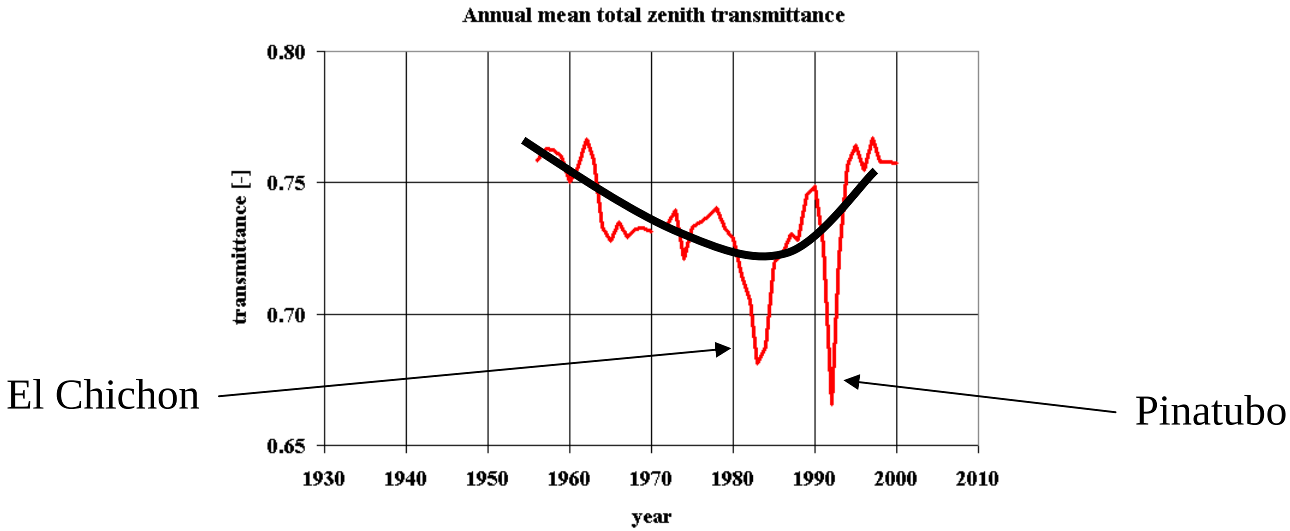

Calanca, 02.05.2006